Transition from Linear to Nonlinear Sputtering of Solid Xenon

Łukasz Dutkiewicz and Roman Pędrys
Institute of Physics, Jagellonian University, ul. Reymonta 4, 30-059 Kraków, Poland

Jørgen Schou
Department of Optics and Fluid Dynamics, Risø National Laboratory, DK-400 Roskilde, Denmark

Kurt Kremer
Institut für Festkörperphysik, KFA Jülich, Germany
(Received 10 December 1993; revised manuscript received 6 March 1995)

Self-sputtering of solid xenon has been studied with molecular dynamics simulations as a model system for the transition from dominantly linear to strongly nonlinear effects. The simulation covered the projectile energy range from 20 to 750 eV. Within a relatively narrow range from 30 to 250 eV, nonlinear features such as high collision densities in the sputtering volume, amorphization of the crystalline structure, and an enhanced emission of low-energy atoms occur gradually.

PACS numbers: 79.20.Nc, 47.20.Ky

Erosion of solids by an ion beam leads to a variety of phenomena. The ejection of target particles (i.e., *sputtering*) as a result of ion bombardment is caused typically by momentum transfer to a target atom that initiates a sequence of collisions so that some atoms in motion eventually leave the solid [1–3]. The behavior of such a collision cascade is critically determined by the density of collisions between the primary particle and the target atoms, and by the binding energy of the atoms to the lattice site. For typical target materials as, e.g., metals, atoms are bound to the lattice site with a binding energy of a few eV. Sputtering of these materials by not too heavy keV ions occurs almost exclusively due to *linear collision cascades*. In a linear cascade each atom set in motion collides with an atom at rest.

A typical nonlinear case occurs for ion bombardment of a frozen gas. Because of the low cohesive energy, the majority of atoms within the primary collision volume are set in motion, and each atom is likely to collide with other moving atoms. Such behavior has been observed experimentally in several cases [4–8] and has also been treated theoretically by a number of authors [9–12]. Solid xenon is particularly appropriate for a study of linear and nonlinear effects in sputtering. The cohesive energy is not too small (160 meV/atom) so that sputtering by incident xenon ions via linear collision cascades *alone* is expected to be produced by experimentally accessible energies around 50 eV. At sufficiently high primary energies, the nonlinear behavior will be dominant.

In the linear cascade regime it is possible to describe the evolution of the system with a linearized Boltzmann equation [3,13]. With enhanced collision density and decreasing cohesive energy of the target, nonlinear effects become increasingly important [9,13,14]. Then, the nonlinear terms in the Boltzmann equation can no longer be neglected.

The present work shows for the first time how it is possible to follow the sputtering process in the same system from a strictly linear to a nonlinear behavior within a relatively narrow range of primary energies with the same method. The study has been performed by molecular dynamics simulations which allow us to deduce important quantities during all stages of the sputtering process [15–17]. Furthermore, the system has the advantage that relevant experimental data are available, and it turns out that the agreement between the calculations and the existing data is good.

Simulations of 20, 30, 60, 100, 250, 400, and 750 eV Xe → Xe bombardment were carried out for an angle of incidence of 0° and 60°. The size of the sample varied from 1536 atoms at 20 eV up to 56 448 atoms at 750 eV (cf. Table I for details). An increased number of target atoms did not influence the results in a significant way.

The target had been equilibrated at $T_{eq} = 15$ K before it was hit by the projectile. After the impact, the energy dissipation from the target to the environment was controlled by the coupling of side and bottom layers

TABLE I. The yields obtained in the simulation of Xe → Xe sputtering. E_0 is the projectile energy, θ is the angle of incidence, Y is the sputtering yield, N_E is the number of simulated events, and N_A is the number of target atoms.

E_0 (eV)	θ	Y	N_E	N_A
20	0°	3.4 ± 0.3	300	1536
30	0°	6.2 ± 0.4	950	1536
60	0°	11.5 ± 2.1	60	2268
100	0°	31.6 ± 3.1	100	2268
250	0°	47.2 ± 3.5	80	6760
250	60°	48.4 ± 2.3	100	6760
400	0°	61.2 ± 17.7	30	20 800
750	0°	168.7 ± 16.3	40	56 448

0031-9007/95/75(7)/1407(4)$06.00

of the simulated sample to a Langevin heat bath of temperature T_{eq} [18]. The strength of the coupling constant corresponded to the heat diffusivity of Xe at 15 K, which equals to 480 $Å^2/ps$.

Since momentum transfers along crystallographic directions are expected to play an important role, a crystalline target was modeled in order to incorporate structure effects. The atoms were arranged in an fcc lattice with a lattice constant of 6.13 Å [19]. The results were averaged over (100), (110), and (111) crystal faces and over the direction and the point of projectile impact relative to crystal orientation. The number of events simulated for a given energy is shown in Table I. All interactions were modeled by the X2 potential due to Barker *et al.* [19], splined with the KrC potential [20] around 1 eV. The potential was cut off at 10.5 Å.

In our molecular dynamics code [21] the velocity Verlet algorithm [22] with variable time step was used to integrate the equations of motion. The time step was adjusted to the maximum allowed displacement, 0.04 Å, per integration step. The atoms were assumed to be sputtered after having crossed a detector plane situated at 12 Å (farther off than the cutoff distance) above the target surface.

The impact of an energetic ion on the surface of a sample initiates collision cascades. Depending on the energy of the incoming projectile, the density of the cascades varies dramatically. In Fig. 1 we show the dilute "linear" cascades produced after a 30 eV projectile impact and the dense system of atoms created after a 250 eV impact. The figure shows side views of the simulated samples at 2 ps after the projectile impact. The radius of the atoms drawn in the figure is proportional to their kinetic energy up to a maximum radius corresponding to the well depth of the interaction potential $U_{pot} = 0.023$ eV. Within a distance of 30 Å from the point of impact, the fraction of atoms with kinetic energy exceeding U_{pot} is, within this region, about 5% for 30 eV and 50% for 250 eV. This means that collisions between moving atoms are very likely to occur in the latter case.

A large number of collisions destroys the crystal structure in the dense collision region. This can be demonstrated by examining the pair correlation function $g(r)$ [15] and the mean square displacement

$$\mathrm{MSD}(r,t) = \sum_{i:|\mathbf{r}_i(t)-\mathbf{r}_{\mathrm{impact}}|\le 30\ \text{Å}} [\mathbf{r}_i(t) - \mathbf{r}_i(0)]^2,$$

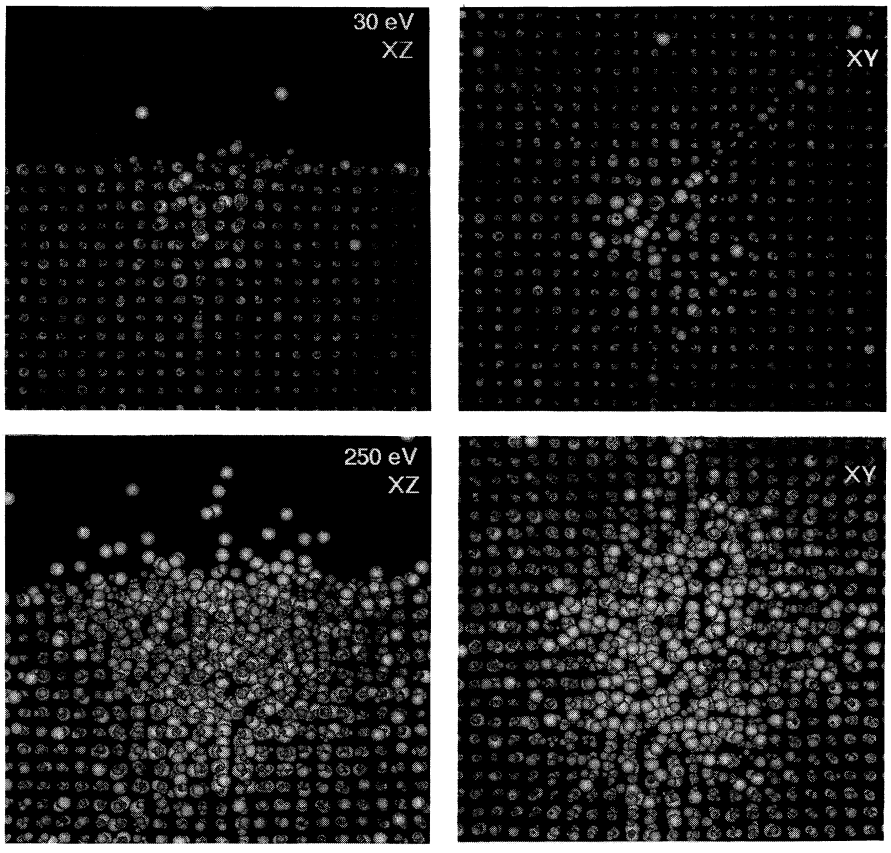

FIG. 1. The state of Xe fcc (100) solid observed 2 ps after 30 and 250 eV Xe projectile impacts. The atoms are visualized as spheres with a radius proportional to their kinetic energy (up to energy $U_{pot} = 0.023$ eV, above which it remains constant). In addition, the spheres are made brighter with increasing energy. The incident projectile is visible as a large, dark sphere. Both top (*XY*) and side views (*XZ*) through all atomic planes of the crystal are shown. Only the central part is shown.

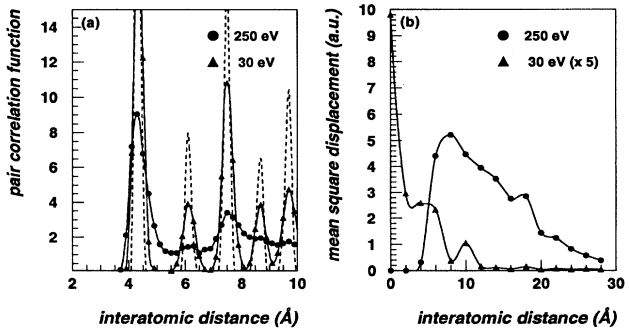

FIG. 2. (a) The pair correlation function of an fcc (100) Xe crystal, determined before (dashed line) and 8 ps after 30 and 250 eV Xe projectile impacts (solid line). (b) Mean square displacement of the atoms from their initial positions, determined 8 ps after the impacts, as a function of distance from the place of impact. In (a) and (b) only the atoms remaining in the solid within a 30 Å radius from the place were taken into account.

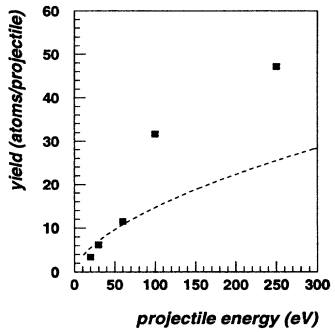

FIG. 3. The sputtering yield obtained from the present simulation (squares) and from linear collision cascade theory (dashes) [13], given as a function of the incident energy.

with $\mathbf{r}_{\text{impact}}$ being the ion impact point on the surface. The plots of MSD($r, t = 8$ ps) for the chosen 30 and 250 eV are shown in Fig. 2(a). The damage produced by the 250 eV impact is much more severe and the damaged volume much larger (about 30 Å diameter) than in the 30 eV case. In Fig. 2(b), $g(r)$ of the bombarded sample (within the 30 Å sphere) before the ion impact and 8 ps after the ion impact is shown. For the 30 eV case we see that $g(r)$ does not change considerably so that the crystal order is conserved after the low-energy impact. For the 250 eV case we get a very different picture: $g(r)$ exhibits a shape characteristic for a liquid with no long-range order. A similar behavior of $g(r)$ was observed by Diaz de la Rubia *et al.* in simulations of keV displacement cascades in Cu and Ni [23]. The structural changes induced by 250 eV bombardment imply the existence of dense collision cascades, characteristic for a nonlinear regime.

The differences observed in the behavior of the solid for 30 and 250 eV impacts strongly influence the experimentally attainable quantities such as the sputtering yield and the energy spectra of ejected particles. In order to check the validity of the calculations performed, we have compared our results with the experimental results. At low bombardment energies, where no experimental data are available, the results have been compared to the linear theory (with KrC stopping cross section) [3], as the observed behavior of our system is dominantly linear. It turns out that both the sputtering yields and the energy spectra of the sputtered atoms at energies up to 60 eV agree well with the linear theory. This is shown in Figs. 3 and 4. The lowest energy at which the sputtering yield for Xe → Xe system is determined experimentally is 750 eV (normal incidence) [6]. The yield of 168 atoms per impact is in reasonable agreement with a value of 112 atoms/ions obtained in Ref. [6]. Also, the energy spectra of the sputtered atoms agree well with experimental measurements [5]. As an example, we present a comparison between a simulated and an experimental energy spectrum for 250 eV at 60° incidence in Fig. 4(c).

The discrepancy between the predictions of the linear theory and the results of the simulation increases with projectile energy; this can be seen in the yields presented in Fig. 3 and in Table I, as well as in the energy spectra presented in Fig. 4(c). However, even at high impact energies a significant contribution from the linear processes exists. Since this contribution comes from atoms sputtered as a result of energetic collision cascades, it should only be present in the flux of atoms ejected soon after the ion impact, i.e., until approximately 2 ps in our case (which is about the time when a dense collision region in the sample is established, as demonstrated in Fig. 1). In order to extract the linear contribution, a double-detector system was established to keep track of

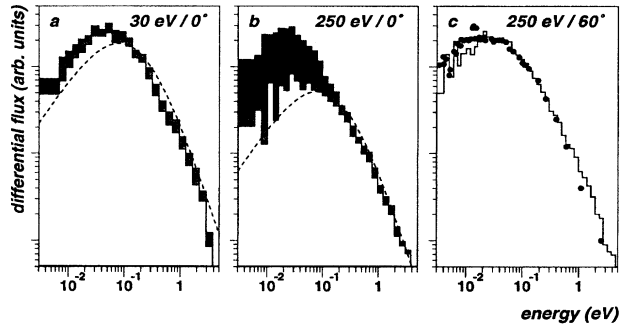

FIG. 4. The simulated energy spectra of atoms sputtered from solid Xe by 30 and 250 eV Xe projectiles. The spectra are shown for various incident energy and angle-of-incidence combinations. (a) and (b) For normal incidence, the spectra taken 2 ps after the ion impact and the total spectra are presented. The difference between the spectrum of atoms sputtered during the first 2 ps after the impact and the spectra formed by all ejected atoms is darkened. The best fit of the Thompson-Sigmund curve [13] is presented by a dashed line. (c) the 60° incidence spectrum is compared with experimental data of Pędrys [5].

the time when a particle was emitted from the surface. This has been implemented as follows: At 3 Å above the target surface, a "trigger" detector was situated; for all atoms crossing this plane the time of crossing was recorded. If the atom passed the second plane at 12 Å, it was assumed to be sputtered, but its emission time was taken from the data recorded by the trigger detector.

Given this information, we could find the number of sputtered atoms vs time of their *emission* for various projectile energies. We can learn from these data that almost 80% of all atoms sputtered with 30 eV projectiles were emitted in the first 2 ps of the duration of the process, compared to approximately 60% for 250 eV bombardment, which means that a significant number of atoms have been sputtered as a result of long-lasting, *nonlinear* processes in the latter case.

The energy spectra of atoms emitted within 2 ps after the 30 eV (or 250 eV) impact are compared to the spectra of all sputtered particles in Figs. 4(a) and 4(b), respectively. Again, it can be seen that the atoms emitted within the first 2 ps for *both 30 and 250 eV* form energy spectra that fit the linear Thompson-Sigmund curve [3]. The total spectrum of atoms sputtered from 30 eV bombardment shows almost no difference with the 2 ps spectra, in contrast to the 250 eV spectra where a significant low-energy part of the spectra is built up as a result of long-lasting nonlinear processes.

In summary, we have identified the transition from a dominantly linear sputtering process at 30 eV and below, up to a strongly nonlinear behavior at 250 eV and above. With increasing primary energy, the nonlinear features are discernable from the relative enhancement of the total yield and from the number of particles emitted with low energy. However, the most striking change can be observed for the behavior of the system in the near-impact volume, which changes from a dilute collision cascade behavior to a dense system of energetic particles in motion. Sputtering of xenon is an ideal case for these types of calculations. The results may be representative for other materials as well, since the energy losses in our system are purely elastic.

This work has been sponsored by the State Committee for Scientific Research, Poland, under Grant No. 22 368 9102, by the Danish Natural Science Research Council, and by the Gemeinschaft zur Förderung von Aufenthalten Polnischer Studierender in der Bundesrepublik Deutschland. The help of U. Felderhof, Th. Fricke, G. Bunsen, and K. Hinsen from RWTH, Aachen, and the help of the OFD Department of Risø National Laboratory for enabling one of us (Ł. D.) to use the computer equipment, as well as fruitful discussions with M. Bubak, are gratefully acknowledged.

[1] *Sputtering by Particle Bombardment I,* edited by R. Behrisch, Topics in Appl. Phys. Vol. 47 (Springer, Berlin, 1981).
[2] *Fundamental Processes in Sputtering of Atoms and Molecules,* edited by P. Sigmund, SPUT '92 (Mat. Fys. Medd. Kgl. Dan., Vindensk, 1993), p. 43.
[3] P. Sigmund, Phys. Rev. **184**, 383 (1969).
[4] H. H. Andersen, SPUT '92 in (Ref. [2]).
[5] R. Pędrys, Nucl. Instrum. Methods Phys. Res., Sect. B **48**, 525 (1990); R. Pędrys (unpublished).
[6] V. Balaji, D. E. David, T. F. Magnera, J. Michl, and H. M. Urbassek, Nucl. Instrum. Methods Phys. Res., Sect. B **46**, 435 (1990).
[7] O. Ellegaard, J. Schou, and H. Sørensen, Europhys. Lett. **12**, 459 (1990); O. Ellegaard, J. Schou, B. Stenum, H. Sørensen, and R. Pędrys, Nucl. Instrum. Methods Phys. Res., Sect. B **62**, 447 (1992).
[8] J. Schou, O. Ellegaard, R. Pędrys, and H. Sørensen, Nucl. Instrum Methods. Phys. Res., Sect. B **65**, 173 (1992).
[9] R. E. Johnson and J. Schou, SPUT '92 in (Ref. [2]), p. 403.
[10] P. Sigmund and C. Claussen, J. Appl. Phys. **52**, 990 (1981); P. Sigmund and M. Szymoński, Appl. Phys. A **33**, 141 (1984).
[11] R. E. Johnson, Int. J. Mass Spectrom. Ion Proc. **78**, 357 (1987).
[12] H. M. Urbassek and K. T. Waldeer, Phys. Rev. Lett. **67**, 105 (1991); K. T. Waldeer and H. M. Urbassek, Nucl. Instrum. Methods Phys. Res., Sect. B **73**, 14 (1993).
[13] P. Sigmund, in *Topics in Applied Physics* (Ref. [1]), p. 9.
[14] B. Stenum, J. Schou, O. Ellegaard, H. Sørensen, and R. Pędrys, Phys. Rev. Lett. **67**, 2842 (1991).
[15] M. P. Allen and D. J. Tildesley, *Computer Simulation of Liquids* (Oxford University Press, New York, 1987).
[16] R. Nieminen, SPUT '92 in (Ref. [2]).
[17] B. J. Garrison and R. E. Johnson, Surf. Sci. **148**, 388 (1984).
[18] T. Schneider and E. Stoll, Phys. Rev. B **17**, 1302 (1978).
[19] J. A. Barker, R. O. Watts, J. K. Lee, T. P. Schafer, and Y. T. Lee, J. Chem. Phys. **61**, 3081 (1974).
[20] W. D. Wilson, L. G. Haggmark J. P. Biersack, Phys. Rev. B **15**, 2458 (1977).
[21] Ł. Dutkiewicz, R. Pędrys, and J. Schou, Europhys. Lett. **27**, 323 (1994).
[22] W. C. Swope, H. C. Andersen, P. H. Berens, and K. R. Wilson, J. Chem. Phys. **76**, 637 (1982).
[23] T. Diaz de la Rubia, R. S. Averback, H. Hsieh, and R. Bendek, J. Mater. Res. **4**, 579 (1989).

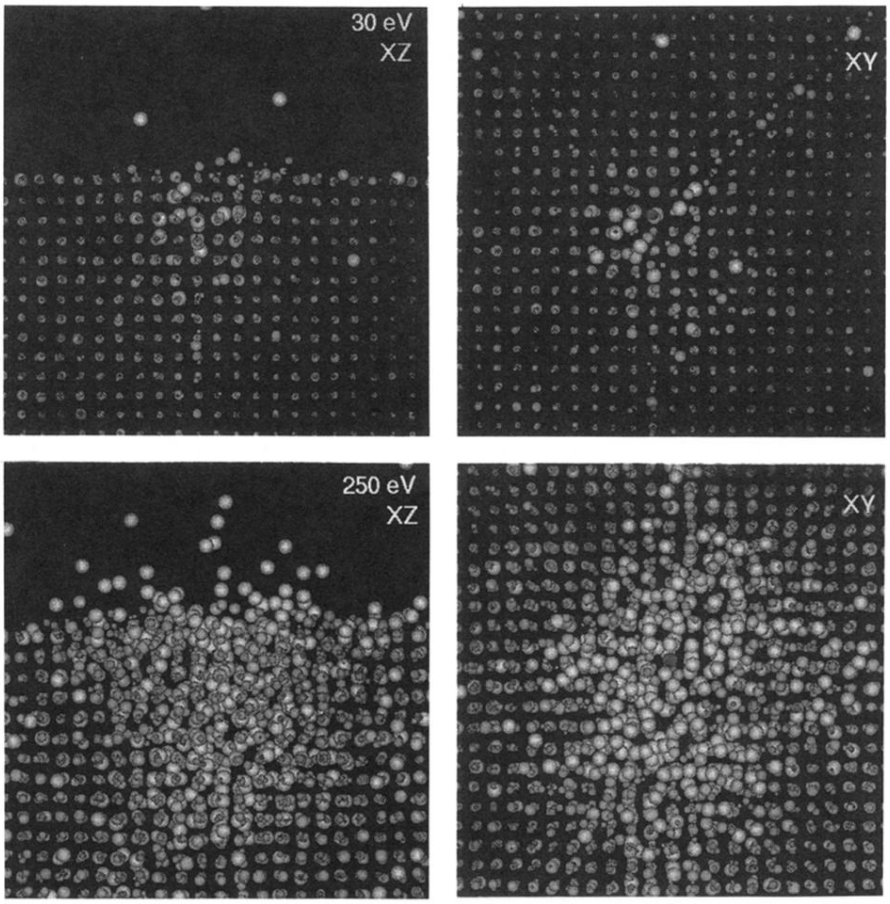

FIG. 1. The state of Xe fcc (100) solid observed 2 ps after 30 and 250 eV Xe projectile impacts. The atoms are visualized as spheres with a radius proportional to their kinetic energy (up to energy $U_{\text{pot}} = 0.023$ eV, above which it remains constant). In addition, the spheres are made brighter with increasing energy. The incident projectile is visible as a large, dark sphere. Both top (XY) and side views (XZ) through all atomic planes of the crystal are shown. Only the central part is shown.